Available online at www.sciencedirect.com
SCIENCE DIRECT®
Thermochimica Acta 410 (2004) 65–71
thermochimica acta
www.elsevier.com/locate/tca

The role of thermal analysis in optimization of the electrochromic effect of nickel oxide thin films, prepared by the sol–gel method: Part II

R. Cerc Korošec*, P. Bukovec

Faculty of Chemistry and Chemical Technology, University of Ljubljana, Aškerčeva 5, 1000 Ljubljana, Slovenia

Received 12 November 2002; received in revised form 4 July 2003; accepted 11 July 2003

Abstract

Thin films and the corresponding xerogels were prepared from nickel acetate precursor using the sol–gel dip-coating technique. The differences in thermal stability of the two forms of samples were studied by dynamic and isothermal thermogravimetry. For thin films, the onset decomposition temperature of acetate groups was 230 °C and for the xerogel 250 °C. During thermal decomposition, the formation of nanosized nickel oxide took place. Carbonate ions, which were formed during thermal decompostion of acetate groups, remained either free or bidentately coordinated to nickel. In situ monochromatic optical transmittance changes showed that an optical stability up to the 100th cycle was already achieved for films heated for 15 min at the isothermal temperature (thermal decompositon 25%). Comparison of the results obtained for nickel sulfate (Part I) and nickel acetate precursors shows that at least two parameters, the precursor used and the degree of thermal treatment, have considerable influence on the thermal stability of the thin film and also on its electrochromic response during the cycling process.

Keywords: TG; NiO thin films; Electrochromism; Sol–gel; Nickel acetate precursor

1. Introduction

Thin films prepared by the sol–gel method from a nickel acetate precursor and thermally treated at 300 °C are electrochemically inert [1]. There are at least two reasons for such behavior. The resistivity of stoichiometric crystalline NiO is large (>10^{13} Ω cm), while the much lower resistivity of semiconducting NiO_x is attributed to impurities and lattice defects [2,3]. Too high processing temperature could therefore lead to formation of a stoichiometric material, which due to its resistivity does not allow proton or hydroxide ion insertion. The intercalation/extraction of one of these species is the basis of the coloration/bleaching process, which takes place during application of the film [4]. The second reason could be an excessively dense structure of the material, which sterically prevents the intercalation of the mentioned species [5].

The electrochromic effect of thin films prepared from a nickel nitrate precursor was also better if they were exposed to a lower temperature, i.e. 250 °C rather than 300 °C or 350 °C [6]. On the other hand, thin films prepared from a nickel sulfate precursor and thermally treated at 300 °C for 15 min exhibited a good electrochromic effect during cycling in an alkaline electrolyte [1,7]. From the isothermal TG curves of thin films, it is obvious that annealing at 270 °C for 60 min is equal to 300 °C for 15 min [8]. The difference in behavior of thin films thermally treated in the same manner but obtained from different precursors makes it essential to perform thermal analysis of thin films for each precursor.

The present work is a continuation of our studies on sol–gel derived nickel oxide films prepared from a $NiSO_4$ precursor [8]. We now present the results of dynamic and isothermal TG analyses, performed on thin films and xerogels prepared from a nickel acetate precursor. The procedure for optimization of the electrochromic effect is carried out in the same manner as described in Part I [8].

2. Experimental

2.1. Preparation of the sol

LiOH (2.0 M) (Kemika, Zagreb, Croatia) was added dropwise with stirring to a 0.5 M solution of nickel acetate

* Corresponding author. Tel.: +386-1-2419-138; fax: +386-1-2419-220.
E-mail address: romana.cerc-korosec@uni-lj.si (R. Cerc Korošec).

0040-6031/$ – see front matter © 2003 Elsevier B.V. All rights reserved.
doi:10.1016/S0040-6031(03)00373-3

(Kemika) until pH 9.0 was reached. The green precipitate was separated from the mother liquor by centrifugation. Then, the slurry was peptized with glacial acetic acid until pH 4.5 was reached. Some water was added to obtain an appropriate viscosity. The sol was then sonicated and filtered.

2.2. Thin film deposition and preparation of the xerogel

An analogous procedure as described in Part I of this article [8] was used to prepare thin films on substrates and the xerogels.

2.3. Instrumental

Measurements of thin films deposited on a microscope-cover glass substrate were performed on a Perkin-Elmer TGA 7 thermoanalyser in the temperature range from 25 up to 400 °C and a dynamic air atmosphere. Measurements of xerogels including isothermal measurements of thin films and xerogels were made on a Mettler Toledo TG/SDTA 851^e instrument. Platinum crucibles (diameter 8 mm) and a heating rate of 5 K min^{-1} were used in dynamic measurements. The initial mass of xerogel was around 6 mg and of the thin film sample (thin *film + substrate*) around 50 mg in dynamic measurements. In isothermal measurements, the furnace was heated to the chosen temperature at 2 K min^{-1}, left at the isothermal temperature for 90 min and then heated up to 350°C at 2 K min^{-1}. For isothermal experiment, the initial masses of thin film samples deposited on microscope-cover glasses were around 100 mg and of xerogel samples were approximately 7 mg. The baseline was in all cases subtracted.

Fourier transform infrared (FT-IR) spectroscopic measurements were made using a Perkin-Elmer System 2000 spectrophotometer with a resolution of 4 cm^{-1}. To obtain transversal optical (TO) modes, the films were deposited on Si wafers.

Powder diffraction data were obtained using a Siemens D5000 X-ray diffractometer with Cu Kα radiation from 5 to 85° 2θ in steps of 0.04° and a time per step 1 s^{-1}.

In situ UV-Vis spectroelectrochemical measurements were performed as described in Part I [8].

3. Results and discussion

3.1. TG analysis

In Fig. 1, dynamic TG curves of amorphous and crystalline xerogels and of a thin film deposited on microscope slide glasses in an air atmosphere are presented. XRD analysis showed that crystalline xerogel is nickel acetate tetrahydrate (PDF No. 26-1282) [9]. Up to 150 °C dehydration took place. During this process, a weight loss of 33.4% for the crystalline and 12.9% for the amorphous xerogel was observed. In case of a sulfate precursor, the weight loss during dehydration was larger for the crystalline xerogel [8]. After 200 °C, thermal decomposition of acetate groups took place. The onset decomposition value for the thin film was 230 °C and for the amorphous xerogel 250 °C. In the temperature range from 200 to 300 °C, the amorphous xerogel lost 44.4% of its weight. On the basis of the EXAFS results, we postulated [8] that probably the same chemical process occurs during thermal decomposition of the thin film and the amorphous powder. From the thin film weight loss from 200 up to 300 °C, we can therefore calculate the initial mass of the thin film (without substrate) and from the difference between the initial mass of the sample and the initial mass of thin film the substrate mass. From this information, the substrate to film mass ratio was determined, and found to be approximately 800.

The thermal decomposition of nickel acetate tetrahydrate was explained in detail in Part I [8]. In Fig. 2, dynamic TG

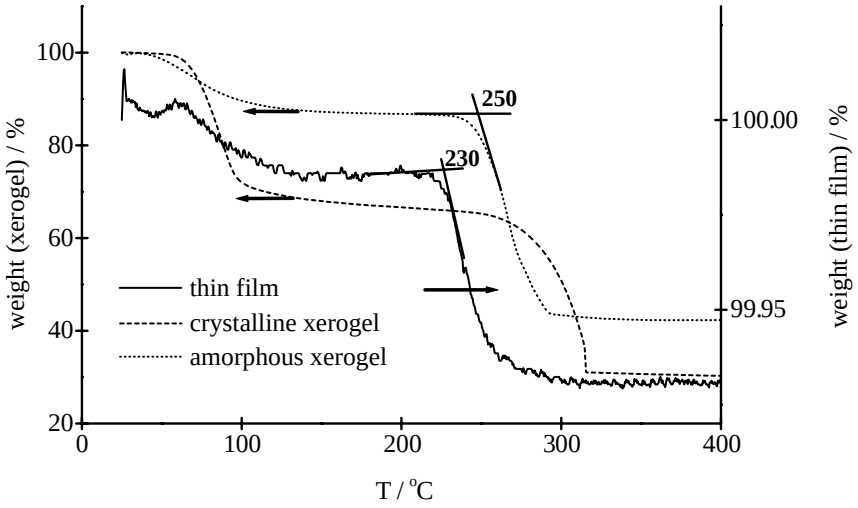

Fig. 1. Dynamic thermogravimetric curves of amorphous and crystalline xerogels—left ordinate—and of a thin film deposited on a microscope-cover glass—right ordinate—in a dynamic air atmosphere.

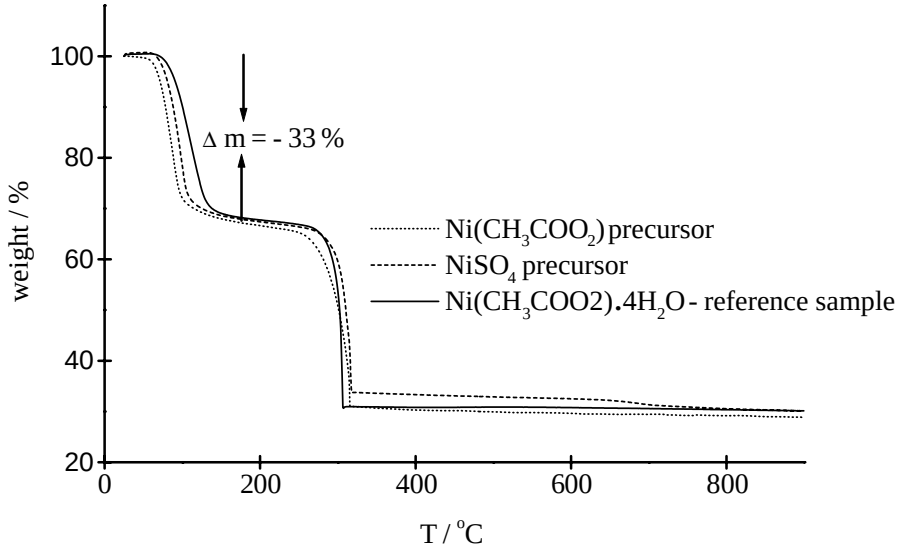

Fig. 2. Dynamic TG curves of crystalline xerogels obtained from either nickel acetate or nickel sulfate precursors and pure nickel acetate (reference sample) in a dynamic air atmosphere. The masses of xerogels were from 6 to 16 mg.

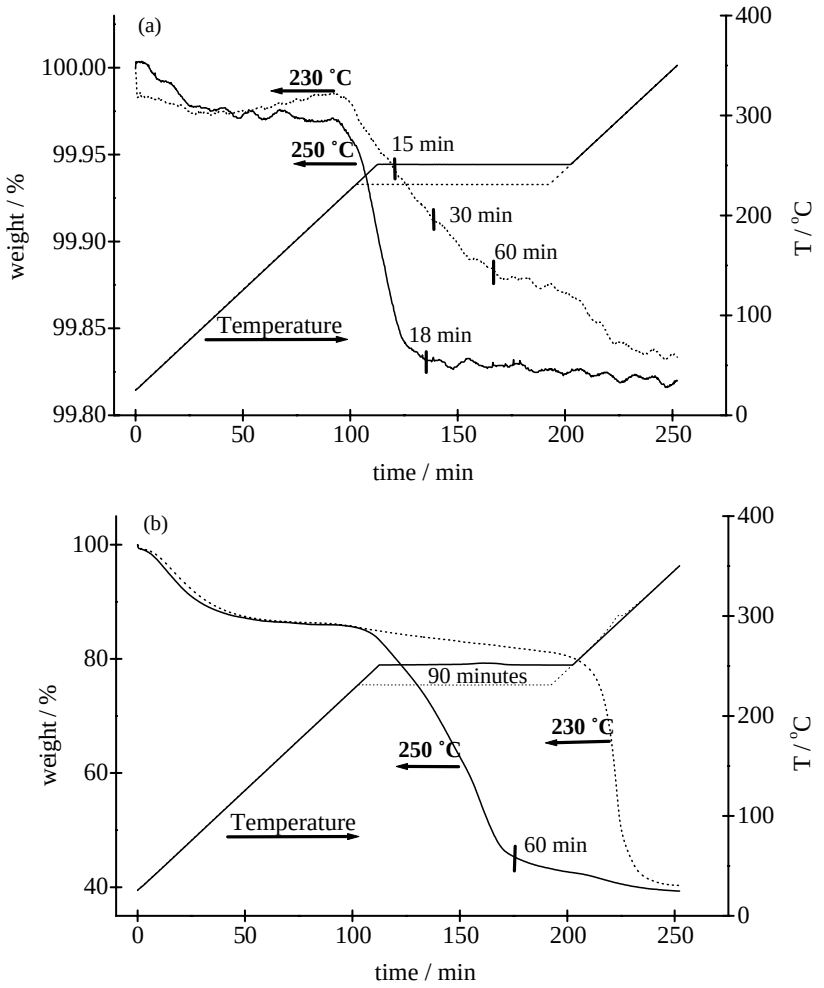

Fig. 3. Isothermal TG curves of a thin film (a) and the corresponding xerogel (b) at 230 and 250 °C.

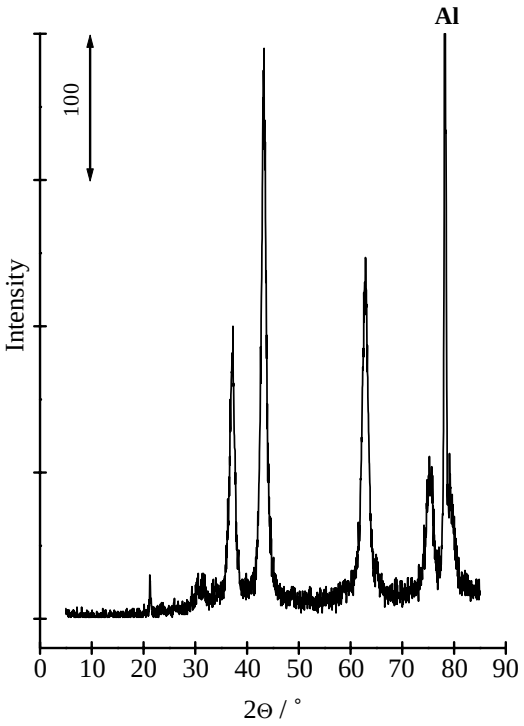

Fig. 4. XRD diffractogram of the amorphous xerogel residue at 300 °C. "Al" denotes the reflection of the aluminum holder.

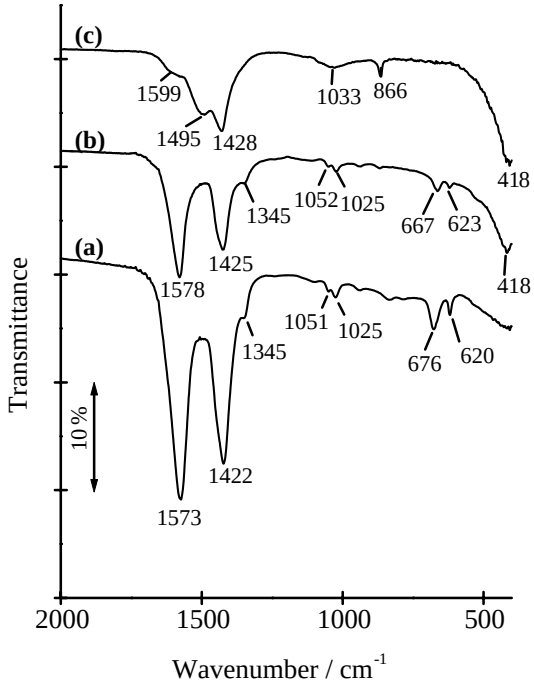

Fig. 5. IR transmittance spectra of the as deposited thin film (a), film thermally treated at 230 °C for 15 min (b) and at 230 °C for 60 min (c).The thin film was deposited on a Si wafer.

curves of crystalline xerogels obtained either from nickel acetate or nickel sulfate precursor are compared with the reference sample (99.9% $Ni(CH_3COO)_2{\cdot}4H_2O$, Aldrich) up to 900 °C.

Isothermal TG curves measured at 230 and at 250 °C for the thin film and the amorphous xerogel are shown in Fig. 3. The isothermal temperatures were chosen on the basis of dynamic measurements (Fig. 1). The thermal decomposition of acetate groups at 230 °C in the thin film sample was 25% after 15 min, 45% after 30 min and 65% after 1 h (Fig. 3a). At 250 °C, decomposition was complete after approximately 20 min. In the amorphous xerogel sample only 8% decomposition was observed after 1 h at 230 °C (Fig. 3b). At 250 °C, the decomposition of acetate groups was 90% after 60 min. On the basis of the isothermal TG curve of the thin film at 230 °C, several thin films can be prepared with different ratios between the nanosized nickel oxide phase, which is formed during the decomposition process (Figs. 4 and 5), and the thermally undecomposed amorphous phase.

3.2. XRD analysis

After thermal decomposition of the acetates, the XRD diffractogram of the residue confirmed the presence of a Bunsenite NiO phase (PDF No. 4-835) [9]. The calculated grain size using the Scherrer formula is approximately 8 nm. The crystallite size of the two residues obtained from the amorphous xerogel after thermal decomposition of acetate groups from either a nickel sulfate or nickel acetate precursor is practically the same.

3.3. IR analysis

In the thermally untreated film (Fig. 5a), the bands at 1573 and 1422 cm^{-1} belong to asymmetric ($\nu_a(COO^-)$) and symmetric ($\nu_s(COO^-)$) vibrations of the acetate group [10]. The vibrations of the methyl group are revealed at 1345, 1051 and 1025 cm^{-1}. The band at 676 cm^{-1} arises from the bending vibration of the acetate group (δ(OCO)), and that at 620 cm^{-1} is attributed to the π(COO) or π(CH) vibration. When the thin film is exposed at 230 °C for 15 min, the intensity of vibrations due to the presence of the acetate group is decreased (Fig. 5b). The new band appearing at 418 cm^{-1} corresponds to the stretching vibration of NiO [11]. The vibrations of carbonate groups appear in the IR spectrum of the film which was heated for 60 min at 230 °C (Fig. 5c). The bands at 1599 and 1033 cm^{-1} correspond to the stretching ($C–O_{II}$) and to ($C–O_I$) vibrations of a bidentately coordinated carbonate ion [12], whereas the vibrations at 1495, 1428 and 866 cm^{-1} belong to vibrations of a free carbonate ion (D_{3h} symmetry) [13]. The results of IR spectroscopy show that during thermal decomposition part of the carbonate ions, which originate from acetate groups, remain either free between the grains of nanosized nickel oxide or bind to the nickel cation via two oxygen atoms.

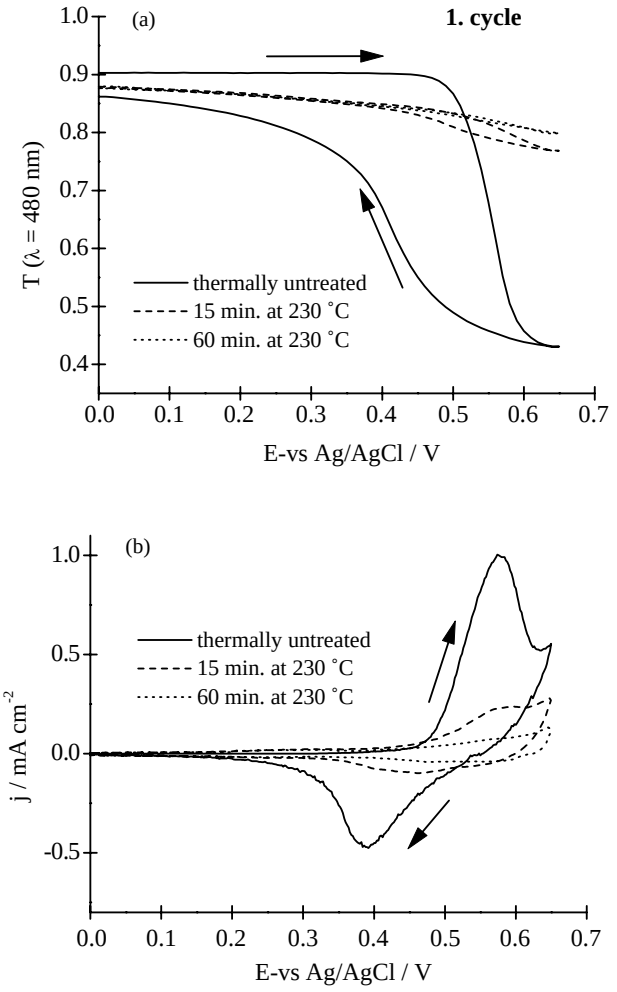

Fig. 6. Monochromatic transmittance changes (a) and cyclovoltammetric curves (b) of nickel oxide films thermally treated to a different extent in 0.1 M LiOH (1st cycle). The thickness of the as deposited film was 25 nm and less than 20 nm for layers thermally treated at 230 °C.

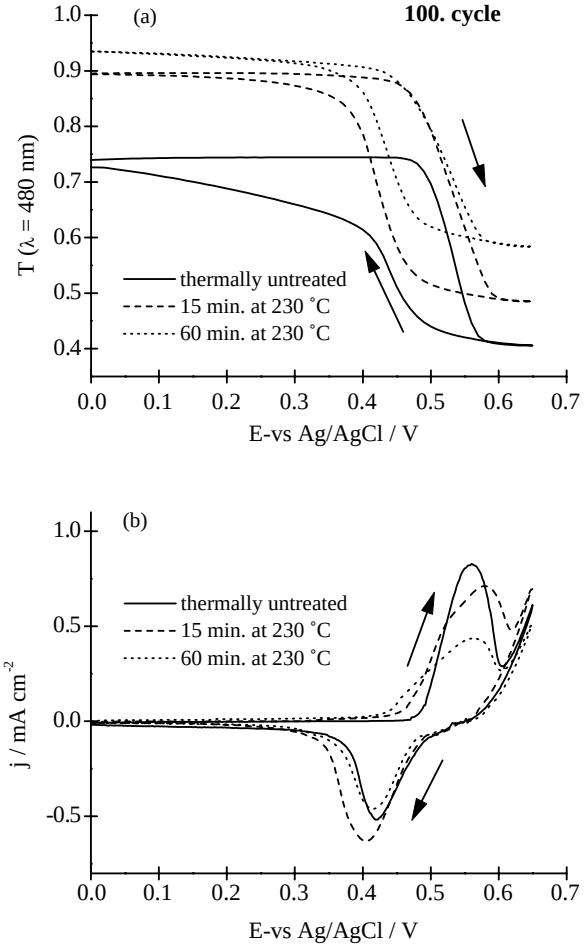

Fig. 7. Monochromatic transmittance changes (a) and cyclovoltammetric curves (b) of nickel oxide films thermally treated to a different extent in 0.1 M LiOH (100th cycle).

Table 1
Position of the anodic and cathodic peaks (E_p), maximal current densities (j_p), the ratio between he anodic and cathodic charge (Q_A/Q_C) and the transmittance value ($\lambda = 480$ nm) at the beginning and at the end of the cycle

	1st cycle		100th cycle	
	Oxidation	Reduction	Oxidation	Reduction
Thermally untreated				
E_p (V)	0.57	0.39	0.56	0.42
j_p (mA cm^{-2})	1.00	−0.47	0.83	−0.52
Q_C/Q_A	0.51		0.53	
T ($\lambda = 480$ nm)	0.903 → 0.431	0.431 → 0.862	0.739 → 0.406	0.406 → 0.726
15 min/230 °C				
E_p (V)	0.58	0.45	0.58	0.41
j_p (mA cm^{-2})	0.23	−0.10	0.71	−0.63
Q_C/Q_A	0.47		0.55	
T ($\lambda = 480$ nm)	0.879 → 0.768	0.768 → 0.877	0.895 → 0.485	0.485 → 0.894
60 min/230 °C				
E_p (V)	–	–	0.56	0.41
j_p (mA cm^{-2})	0.12	−0.04	0.43	−0.46
Q_C/Q_A	1.00		0.53	
T ($\lambda = 480$ nm)	0.876 → 0.799	0.799 → 0.879	0.935 → 0.539	0.539 → 0.934

3.4. In situ optical and cyclovoltammetric results

The optical transmittance changes at $\lambda = 480$ nm during cyclovoltammetric measurements for a thermally untreated film and for films kept at 230 °C for 15 or 60 min are presented in Fig. 6 (1st cycle) and Fig. 7 (100th cycle). In the thermally untreated film, oxidation of Ni^{2+} ions causes a large change in transmittance, i.e. from 0.90 at the beginning of the cycle to 0.43 at the end of the anodic scan, but the reduction process does not bleach the layer to the initial value. A decrease in the transmittance value of the film in its bleached state of 4.1% is observed. Both thermally treated films exhibit very little color change during the oxidation process in the first cycle. The values are given in Table 1. According to the results obtained from in situ optical measurements the current density of the thermally untreated film is large compared with the other two films. Up to the 100th cycle, the anodic current density of the thermally untreated film diminishes and the cathodic current density becomes a little larger, but the transmittance is only 0.74 in the bleached state. For both thermally treated films, current densities become approximately three times larger, and the observed transmittance change during the oxidation/reduction process is 40%. The initial transmittance value for the film thermally treated at 230 °C for 60 min is even 6% larger than at the beginning of cycling. Reversibility of the optical process for these films is achieved before the thermal decomposition of acetate groups is finished (in the film thermally treated at 230 °C for 15 min, this means only 25% decomposition ensures stability up to 100th cycle).

4. Conclusions

In the conclusion also the results of Part I [8] are summarized together with the results of this article.

Time dependence of the isothermal weight loss of thin films prepared from nickel sulfate or nickel acetate precursor via sol–gel route helps us to prepare thin films with different stoichiometry between thermally undecomposed amorphous phase and nanosized nickel oxide. Isothermal temperature can be chosen on the basis of dynamic measurements. It is 270 °C for thin films prepared from $NiSO_4$ precursor [8] and 230 °C in case of $Ni(CH_3COO)_2$ precursor. Results obtained for the corresponding xerogels could not be used because higher decomposition temperature was determined in the latter case.

During isothermal treatment, the combustion of acetate groups, which are present in both samples (Ni-sulfate, Ni-acetate precursor) due to peptisation of the gel with acetic acid, takes place and nickel oxide is being formed.

It is evident from in situ spectroelectrochemical measurements that the ratio between thermally undecomposed amorphous phase and nickel oxide is decisive for the electrochromic response and stability of these films during cycling in alkaline electrolyte.

Before isothermal treatment, the optical response shows irreversibility for the process $Ni^{2+} \leftrightarrow Ni^{3+}$. But different electrochromic behaviors were observed for sulfate and acetate thin films isothermally treated to the similar extent. In the case of a sulfate precursor, the best properties up to 100th cycle are possessed by a thin film, in which thermal decomposition of acetate groups is complete (60 min at 270 °C). The change in transmittance at $\lambda = 480$ nm for this film in the 100th cycle is 46%. For the acetate precursor optical reversibility is already achieved in a film thermally treated at 230 °C for 15 min (25% decomposition). The monochromatic transmittance change is 40% in the 100th cycle, but greater differences between these two films are observed at the beginning of the cycling, where the optical response of the latter is very small (11%). The initial response in case of the sulfate precursor is 26%. The electrochemical mechanism at the beginning of the cycling process is most likely different for thin films prepared from $NiSO_4$ or $Ni(CH_3COO)_2$ precursors and further studies should be made in order to elucidate this difference.

The grain size of the xerogel residues after thermal decomposition is nearly the same for both precursors (from 8 to 9 nm), so we exclude that grain size causes the observed differences. Most probably the anions are responsible for them. IR analysis shows that in case of sulfate precursor, sulfate ions remain monodentately bonded to nickel after thermal decomposition of acetates. On the other hand, the carbonate ions formed during thermal decomposition of the mentioned species bind bidentately to nickel, or remain free in the structure in the case of an acetate precursor.

The role of dynamic and isothermal TG analysis in the optimization procedure of the described thin films is that it enables the determination of the processing temperature. Optimal time of isothermal heat-treatment can be determined using additional sprectoelectrochemical measurements. From the shape of isothermal TG curves (time dependence) one can propose the duration of heat-treatment at which makes is essential to test electrochromic response.

Acknowledgements

This work was supported by Grant PO-0508-0103 from the Ministry of Education, Science and Sport of the Republic of Slovenia.

References

[1] A. Šurca, B. Orel, B. Pihlar, P. Bukovec, J. Electroanal. Chem. 408 (1996) 83.
[2] D. Adler, J. Feinleib, Phys. Rev. B 2 (1970) 3112.
[3] A.F. Wells, Structural Inorganic Chemistry, fourth ed., Clarendon Press, Oxford, 1975, p. 445.
[4] A. Agrawal, H.R. Habibi, R.K. Agrawal, J.P. Cronin, D.M. Roberts, R.S. Caron-Popowich, C.M. Lampert, Thin Solid Films 221 (1992) 239.

[5] R. Cerc Korošec, P. Bukovec, J. Therm. Anal. Catal. 56 (1999) 587.
[6] T. Miki, K. Yoshimura, Y. Tai, M. Tazawa, P. Jin, S. Tanemura, in: Proceedings of the Third IUMRS International Conference on Advanced Materials, Tokyo, Japan, 31 August–4 September 1993 (article No. KP12).
[7] A. Šurca, B. Orel, R. Cerc Korošec, P. Bukovec, B. Pihlar, J. Electroanal. Chem. 433 (1997) 57.
[8] R. Cerc Korošec, P. Bukovec, B. Pihlar, J. Padež nik Gomilšek, Thermochim. Acta 402 (2003) 57.
[9] X-Ray Powder Diffraction File, JCPDS-ICDD, Nowtown, ZDA, 1999.
[10] K. Nakamoto, Infrared and Raman Spectra of Inorganic and Coordination Compounds, Part B, fifth ed., Wiley, New York 1997, pp. 59–60.
[11] C. Faure, C. Delmas, M. Fouassier, J. Power Sources 35 (1991) 279.
[12] K. Nakamoto, Infrared and Raman Spectra of Inorganic and Coordination Compounds, Part B, fifth ed., Wiley, New York 1997, pp. 84–86.
[13] K. Nakamoto, Infrared and Raman Spectra of Inorganic and Coordination Compounds, Part A, fifth ed., Wiley, New York 1997, p. 182.